催 化 学 报
2012 Chinese Journal of Catalysis Vol. 33 No. 2

文章编号: 0253-9837(2012)02-0290-08 国际版 DOI: 10.1016/S1872-2067(11)60332-X 研究论文: 290~297

快速功能化碳纳米管载 Pt 催化剂的醇氧化性能

尹诗斌[1,2,a], 朱强强[2], 强颖怀[2], 罗 林[1,2,b]

[1]中国矿业大学低碳能源研究院, 江苏徐州 221116

[2]中国矿业大学材料科学与工程技术学院, 江苏徐州 221116

摘要: 采用 HF 刻蚀及交替微波加 H_2O_2 相结合的方法进行快速功能化碳纳米管 (CNTs), 应用红外光谱、拉曼光谱和透射电镜等方法详细考察了 CNTs 及其载 Pt 催化剂的物化性质, 并采用循环伏安法、线性电流扫描法和计时电流法考察了所得催化剂的电化学性能. 结果表明, CNTs 经过HF刻蚀和交替微波 H_2O_2 双重处理后更适合用作催化剂载体, 以 10s-on/20s-off 加热 5 次所得 CNTs 载 Pt 催化剂显示出最佳的催化性能. 这可归因于处理后的 CNTs 表面含有丰富的微孔及含氧官能团, 能有效增强 Pt 颗粒及 CNTs 间的相互作用.

关键词: 燃料电池; 碳纳米管; 功能化; 交替微波法; 甲醇氧化

中图分类号: O643 **文献标识码**: A

收稿日期: 2011-08-29. 接受日期: 2011-10-28.

[a]通讯联系人. 电话: (0516)83883235; 传真: (0516)83883501; 电子信箱: shibinyin@126.com

[b]通讯联系人. 电话/传真: (0516)83883501; 电子信箱: obingye@gmail.com

基金来源: 国家自然科学基金青年基金(21106178); 徐州市科技项目(XJ11B009); 徐州市多晶硅与光伏能源技术专项(6AT102092); 中央高校基本科研业务费专项资金(2011QNA21); 材料复合新技术国家重点实验室(武汉理工大学)开放基金(2012-KF-13).

本文的英文电子版(国际版)由Elsevier出版社在ScienceDirect上出版(http://www.sciencedirect.com/science/journal/18722067).

Functionalized Carbon Nanotubes as Pt Catalyst Supports in Methanol Oxidation

YIN Shibin[1,2,a], ZHU Qiangqiang[2], QIANG Yinghuai[2], LUO Lin[1,2,b]

[1]*Low Carbon Energy Institute, China University of Mining and Technology, Xuzhou 221116, Jiangsu, China*

[2]*School of Materials Science and Engineering, China University of Mining and Technology, Xuzhou 221116, Jiangsu, China*

Abstract: An efficient method for the functionalization of carbon nanotubes (CNTs) is presented, which uses the HF corrosion and intermittent microwave heating (IMH) H_2O_2 solution. The Fourier transform infrared spectroscopy, Raman spectroscopy, and transmission electron microscopy are used to investigate the physicochemical properties of the CNTs and the prepared catalysts thereof. Cyclic voltammetry, liner current sweeping measurements, chronoamperometry measurements are employed to study the performance of the prepared catalysts. CNTs further treated with IMH H_2O_2 solution (10s-on/20s-off, over five cycles) can be used as catalyst support, and exhibit significantly improved performance towards methanol oxidation in comparison with other modified CNTs. The results represent a novel approach to functionalize CNTs in a simple and economic way. The method can also be applied in the mass production of nanosized materials.

Key words: fuel cell; carbon nanotube; functionalization; intermittent microwave heating method; methanol oxidation

Received 29 August 2011. Accepted 28 October 2011.

[a]*Corresponding author. Tel: +86-516-83883235; Fax: +86-516-83883501; E-mail: shibinyin@126.com*

[b]*Corresponding author. Tel/Fax: +86-516-83883501; E-mail: obingye@gmail.com*

This work was supported by the National Natural Science Foundation of China (NSFC) (21106178), the Scientific Research Foundation of Xuzhou (XJ11B009), the Polysilicon and Photovoltaic Energy Technology of Xuzhou (6AT102092), the Fundamental Research Funds for the Central Universities (2011QNA21), and the State Key Laboratory of Advanced Technology for Materials Synthesis and Processing (Wuhan University of Technology) (2012-KF-13).

English edition available online at Elsevier ScienceDirect (http://www.sciencedirect.com/science/journal/18722067).

Carbon nanotubes (CNTs) attract increasing interest as catalyst supports for low temperature fuel cells, due to their unique physicochemical properties, such as relatively high electrical conductivity and corrosion resistance in both acidic and basic media [1–3]. However, owing to their almost perfect structure, it remains a challenge to uniformly deposit metallic particles on the inert CNTs surface. Consequently, great efforts have been devoted to CNTs surface functionalization, to enhance their activity and the interactions between the CNTs and the metallic particles. Techniques include, modifying CNTs with polymers [4,5], enlarging their surface area with KOH [6,7], and chemical treatment with agents such as O_3, HCl, H_2SO_4, and HNO_3 [8,9]. CNTs surfaces can also be etched or functionalized with amine, carboxyl, and/or sulfone groups [10,11]. Liu et al. [12] employed a concentrated H_2SO_4/HNO_3 mixture to cut highly entangled CNTs into shorter lengths, and thus produced numerous carboxyl groups at the open ends. Zhang et al. [8] investigated the efficiency of chemical oxidation upon the structure of CNTs using a range of oxidants. The pretreatment of CNTs may be necessary to finely disperse Pt particles on the surface. However, the above mentioned methods are usually time-consuming, which make the procedures difficult to scale-up. Meanwhile, the treated CNTs tend to be hydrophilic, rendering them hard to filter. Therefore, to functionalize CNTs on a large scale, a time-saving and efficient method needs to be developed.

HF-treated CNTs supported Pt catalysts show an enhanced activity and stability towards alcohol oxidation [13,14]. Microwave irradiation has also been widely used for catalyst synthesis, due to its unique advantages in terms of heating efficiency and capacity [15,16]. In previous studies [17], we have combined the advantages of HF corrosion and intermittent microwave heating (IMH) to modify CNTs as catalyst supports. The modified CNTs supported Pt catalysts show an improved activity towards the oxygen reduction reaction compared with otherwise treated CNTs. Herein, CNTs functionalized with a IMH H_2O_2 solutions are investigated in detail as catalyst supports, and their performance towards methanol oxidation is studied.

1 Experimental

1.1 Carbon nanotubes pretreatment

The proposed mechanism for CNTs modification is shown in Fig. 1. The HF solutions are used to make defects on the surface of the pristine CNTs. The IMH H_2O_2 solution is then employed to produce functional groups upon the defects generated in the first step. Finally, the obtained CNTs are used as catalyst supports.

CNTs with diameters of 10–20 nm and purities >95% (Shenzhen Nanotech. Co., Ltd., China) were used as received. CNTs were initially treated with a HF solution as follows [14]: CNTs (1.0 g) were added to a 40 wt% HF solution (50 g) under continuous stirring for 6 h at room temperature. The treated CNTs were rinsed with neutral deionized water and dried at 353 K under vacuum for 24 h.

A portion of the treated CNTs was further treated with IMH H_2O_2 solutions as follows: CNTs (500 mg) were added

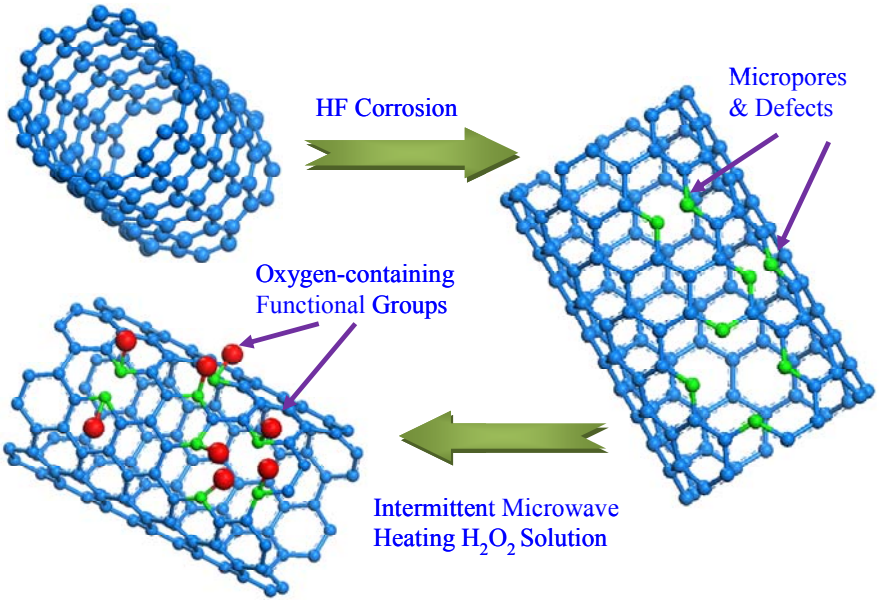

Fig. 1. Proposed mechanism for CNTs modification through combined HF etching/IMH methodology.

to a 10.0 ml 30 wt% H_2O_2 solutions, and after stirring for 10 min, the mixture was microwave heated via a pulsing method (10s-on/10s-off, 10s-on/20s-off, and 10s-on/30s-off for five cycles). The resulting black samples were denoted as CNTs-1, CNTs-2, and CNTs-3. The CNTs treated with HF only were denoted as CNTs-HF.

1.2 Catalyst preparation

The 20 wt% Pt/CNTs catalysts were easily and rapidly prepared using the IMH method as follows [15,16,18]: chloroplatinic acid, the starting precursor, was well mixed with ethylene glycol (EG) in an ultrasonic bath. CNTs were then added into the mixture. The pH adjusted to more than 10 using an NaOH/EG solution, and a well-dispersed slurry was obtained upon stirring and ultrasonication for 15 min. Thereafter, the slurry was microwave-heated 5s-on/5s-off over several cycles. Hydrochloric acid was then added. The resulting black solid samples were filtered, washed and dried at 353 K for 12 h in a vacuum oven. The corresponding catalysts are denoted as Pt/CNTs-1, Pt/CNTs-2, Pt/CNTs-3, and Pt/CNTs-HF.

1.3 Catalyst characterization

Fourier transform infrared spectroscopy (FT-IR) measurements were carried out on all the CNTs samples using a Nicolet 5700 spectrometer (Thermo, USA). The Raman spectroscopy measurements were performed on a Renishaw Raman spectrometer (Renishaw Corp., UK), using a He/Ne laser at a wavelength of 514.5 nm. X-ray powder diffraction (XRD) measurements were carried out on a D/Max-III (Rigaku Co., Japan), using Cu K_α radiation (λ = 0.15406 nm), and operating conditions set to 40 kV and 20 mA. The 2θ angular regions between 20° and 90° were explored at a scan rate of 10°/min and the 64°–72° angle range was finely scanned at 1°/min, to obtain the Pt crystal size according to the Scherrer formula [19]. Transmission electron microscopy (TEM) investigations were carried out on a JEOL JEM-2010 (HR) at 200 kV, to interrogate the particle size distribution of Pt within the catalysts. The histograms for the prepared catalysts were made by randomly measuring more than 300 particles.

All electrochemical measurements were conducted on a PARETAT 2273 (Princeton Applied Research, USA) instrument in a thermostatically-controlled standard three-electrode cell at room temperature, adopting a saturated calomel electrode (SCE) and a platinum foil (1 cm × 1 cm) as the reference electrode and counter electrode, respectively. A glass carbon (GC) disk electrode with diameter of 5.0 mm was used as the substrate for the catalyst thin film in the electrochemical measurements. The thin film catalyst layer was prepared as the working electrode as follows: a mixture containing 5.0 mg catalyst, 1.8 ml ethanol and a 0.2 ml Nafion solution (5 wt%) was dispersed in a ultrasonic bath for 10 minutes to afford a well-dispersed ink. The catalyst ink was then quantitatively transferred onto the surface of a GC electrode using a micropipette. This was dried under an infrared lamp to obtain a catalyst thin film. The estimated catalyst loading was kept constant at 0.13 mg/cm^2 in this study. Cyclic voltammograms (CVs) were collected in 0.5 mol/L H_2SO_4 aqueous solutions, with and without nitrogen saturated 1.0 mol/L CH_3OH. All potentials are quoted in reference to the SCE.

2 Results and discussion

The surfaces of the CNTs were characterized using FT-IR and the corresponding results are displayed in Fig. 2. The peaks at 1380 and 1635 cm^{-1} are assigned to the aromatic C=C stretching vibration and COOH group, respectively. The peak at 1730 cm^{-1} is assigned to the C=O– stretching vibration within the COOH group. These peaks only appear after the CNTs are further modified with the IMH H_2O_2 solutions. It can therefore be deduced that the CNTs have been successfully functionalized by the H_2O_2 solution with high temperature treatment. The corrosive action of the H_2O_2 can be attributed to its strong oxidizing nature, especially under the microwave conditions. Microwave heating can rapidly heat the reaction system to a relatively high temperature. It is well known that in catalyst supports, oxygen-containing groups on the CNTs are beneficial because they enhance the hydrophilicity of the CNTs. This improves the dispersion of the catalysts. Meanwhile, they can also stabilize the metallic particles by enhancing the bonding interactions between the metallic particles and the CNTs [7,17].

To further investigate the surfaces of the CNTs with dif-

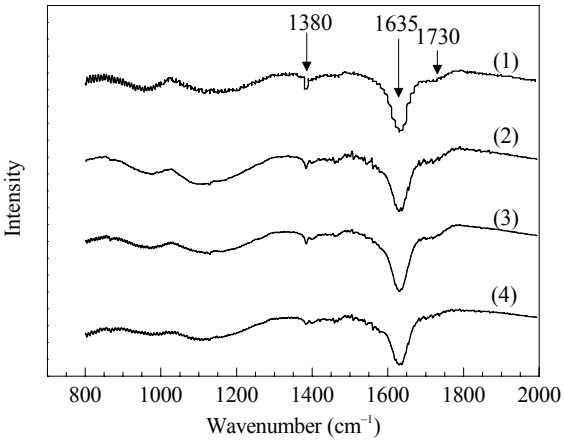

Fig. 2. FT-IR spectra for CNTs-1 (1), CNTs-2 (2), CNTs-3 (3), and CNTs-HF (4).

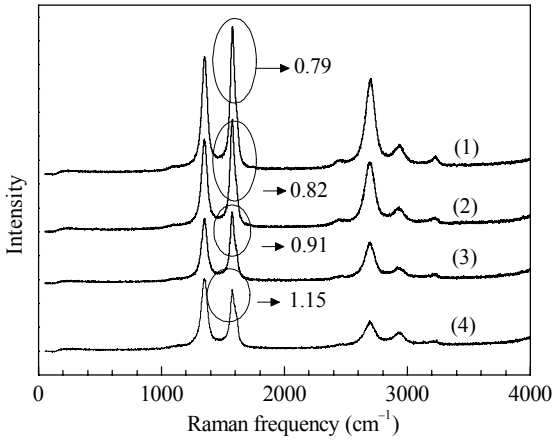

Fig. 3. Raman spectra of CNTs-1 (1), CNTs-2 (2), CNTs-3 (3), and CNTs-HF (4).

ferent pretreatments, Raman spectroscopy was employed and the specific results are shown in Fig. 3. The samples share similar Raman scattering patterns. The peak at 1340 cm^{-1} is assigned to disordered graphite (D-line), and the peak at 1595 cm^{-1} corresponds to the splitting of the E_{2g} stretching mode of graphite. This reflects the structural intensity of the sp^2-hybridized carbon atom, denoted as the G-line. The intensity ratio between the D-line and the G-line can be used as an indicator for the structural integrity of the sp^2-hybridized carbon atoms [20]. Based on the Raman curves, the intensity ratio of the D-line to the G-line is 0.79, 0.82, 0.91, and 1.15 for CNTs-1, CNTs-2, CNTs-3, and CNTs-HF, respectively. The CNTs-HF exhibits the lowest graphitization degree, which can be attributed to defects brought about by the HF [13]. Further treating the CNTs-HF with IMH H_2O_2, the graphitization degree increases. The high temperatures during the microwave treatment may consume portions of the disordered graphite. Meanwhile, the graphitization degree decreases with the relaxation time. This is understandable, because the longer relaxation time lead to relatively lower temperatures. On the other hand, shorter microwave irradiation off time can lead to a relatively higher temperature. Throughout this process, the disordered graphite is oxidized and decomposed, thus increasing the graphitization degree within the CNTs. There are levels of oxygen-containing functional groups on the surfaces of the CNTs, after further treatment with IMH H_2O_2 [17,21], as confirmed from the FT-IR results. This is consistent with the above conclusion.

Figure 4 presents the XRD results for the prepared catalysts. As displayed in the spectra, all the samples show the typical characteristics of a crystalline Pt face centered cubic *fcc* structure. The diffraction peaks at 2θ = 39.6°, 46.3°, 67.4°, and 81.6° are assigned to the (111), (200), (220), and (311) facets of Pt, respectively. The fitted (220) plane is used to calculate the crystal size of Pt according to the Scherrer formula [19]. The average crystal size for Pt/CNTs-1, Pt/CNTs-2, Pt/CNTs-3, and Pt/CNTs-HF is 3.6, 3.3, 2.8, and 2.9 nm, respectively. This could be attributed to the existence of micropores and defects, which would increase the contact area between the Pt particles and the CNTs. This could efficiently inhibit the agglomeration of Pt particles [13]. Therefore, the Pt/CNTs-HF have the smallest crystal size. On the other hand, the level of micropores and defects would be consumed upon further treatment with IMH H_2O_2. Consequently, the crystal size for the Pt deposited on CNTs-1, CNTs-2, and CNTs-3 is larger than that for CNTs-HF.

The TEM micrographs and corresponding particle size distribution histograms for Pt/CNTs-2 and Pt/CNTs-HF are given in Fig. 5. As shown below, the Pt particles are uniformly distributed on both catalysts. The Pt contents as verified by inductively coupled plasma atomic emission spectroscopy (ICP-AES, Perkin-Elmer, Germany) are 83.51%, 83.97%, 83.66%, and 77.59% for Pt/CNTs-1,

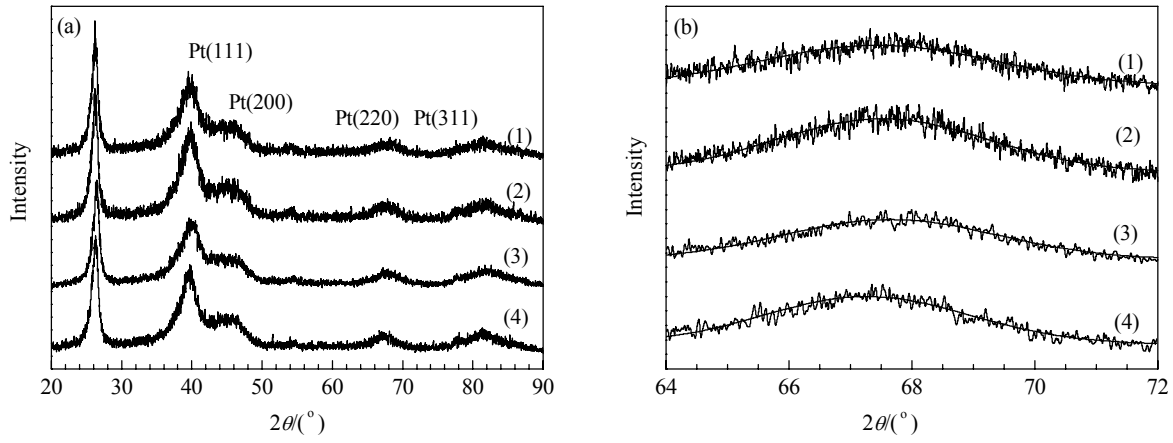

Fig. 4. XRD patterns for Pt/CNTs-1 (1), Pt/CNTs-2 (2), Pt/CNTs-3 (3), and Pt/CNTs-HF (4) at a scan rate of 10°/min (a) and the corresponding Pt (220) peaks at a scan rate of 1°/min (b).

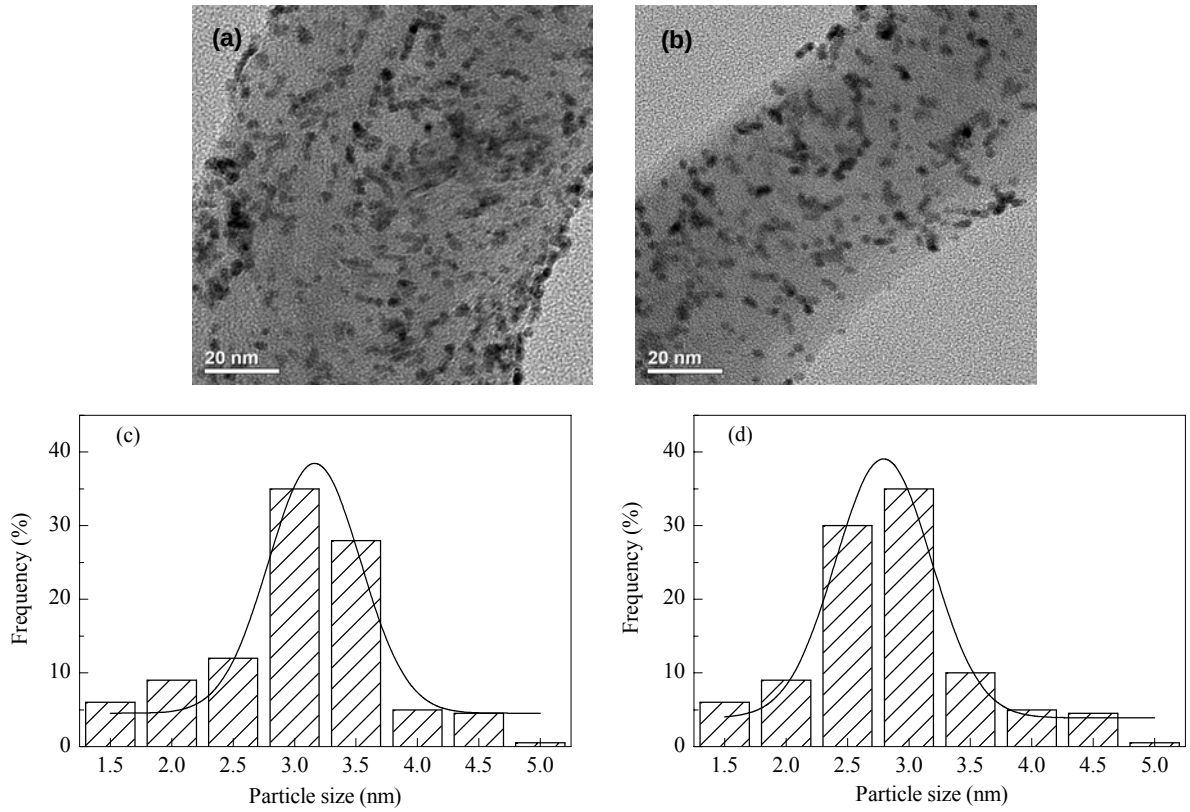

Fig. 5. TEM images for Pt/CNTs-2 (a) and Pt/CNTs-HF (b), and the corresponding particle size distribution histograms for Pt/CNTs-2 (c) and Pt/CNTs-HF (d).

Pt/CNTs-2, Pt/CNTs-3, and Pt/CNTs-HF, respectively. This means that further treatment of the CNTs with IMH H_2O_2 favors the deposition of Pt particles. This may be attributed to the large number of oxygen-contain functional groups on the surface of CNTs-2, which can enhance the interactions between the Pt particles and the CNTs. Moreover, based on the 300 particles measured in random regions, the average particle sizes are estimated to be 3.2 and 2.8 nm for the Pt/CNTs-2 and Pt/CNTs-HF, respectively.

The methanol oxidation performance of the prepared catalysts have been evaluated. Figure 6 shows the CV curves for the catalysts in aqueous 0.5 mol/L H_2SO_4, with and without 1.0 mol/L CH_3OH. Upon integrating the hydrogen adsorption/desorption charges according to the CV curves in Fig. 6(a), the electrochemical surface areas (ESA) of catalysts can be calculated. The charges, Q_H, for Pt/CNTs-1, Pt/CNTs-2, Pt/CNTs-3, and Pt/CNTs-HF are 4.50, 4.73, 4.04, and 3.35 mC/cm^2. The Pt/CNTs-2 have the

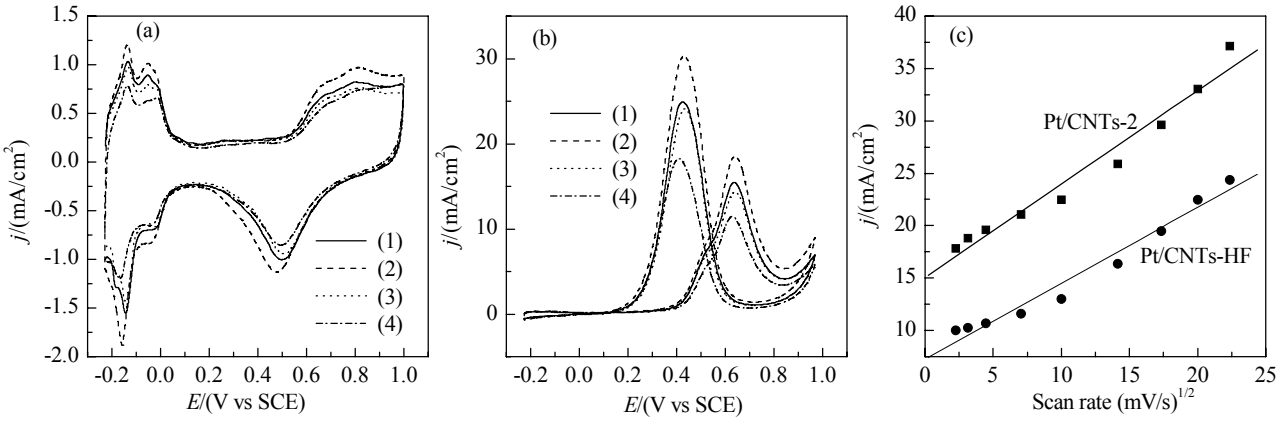

Fig. 6. The CV curves for Pt/CNTs-1 (1), Pt/CNTs-2 (2), Pt/CNTs-3 (3), and Pt/CNTs-HF (4) in 0.5 mol/L aqueous H_2SO_4 without (a) and with (b) 1.0 mol/L CH_3OH at 298 K and plots for the peak current density as a function of the square root of the scan rate for Pt/CNTs-2 and Pt/CNTs-HF (c).

largest ESA, which is 41.19% higher than those measured for Pt/CNTs-HF. The corresponding peak current densities for the methanol oxidation are proportional to the ESA, as shown in Fig. 6(b). The Pt/CNT-2 exhibits the best activity and the specific peak current density is 41.65% higher than that for Pt/CNTs-HF.

We also integrated the anodic peak density for methanol oxidation during the forward potential cycles at different scan rates. The relationship between peak current density and scan rate for Pt/CNTs-2 and Pt/CNTs-HF are displayed in Fig. 6(c). The peak current density for both catalysts increases with increasing scan rate. However, the Pt/CNTs-2 has a larger slope compared with Pt/CNTs-HF and shows a better activity towards methanol oxidation.

The effect of temperature on the electrode was studied using Tafel plots with a scan rate of 1 mV/s. Figure 7(a) summarizes the effects of temperature on the electrode activity. The over-potential at the same current density decreases with increasing temperature. The exchange current densities, j^0, at different temperatures are obtained by extrapolating the linear Tafel lines to where the over-potential equals zero. j^0 is then plotted against $1/T$, as shown in Fig. 7(b). The activation free energy can then be calculated according to the Arrhenius formula [22]:

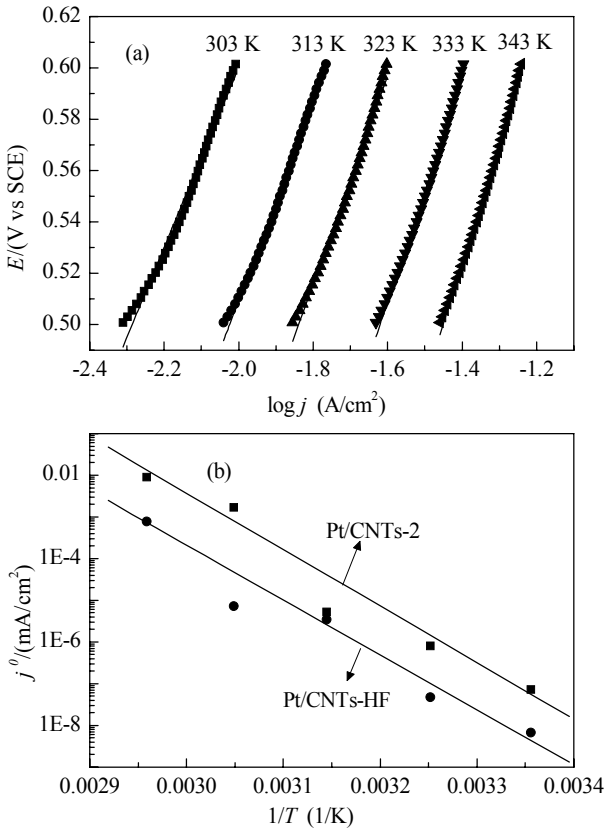

Fig. 7. Tafel plots for the methanol oxidation on the Pt/CNTs-2 (a) and j^0–$1/T$ plots for the methanol oxidation on Pt/CNTs-2 and Pt/CNTs-HF in 0.5 mol/L aqueous H_2SO_4 + 1.0 mol/L CH_3OH (b).

$$\mathrm{Log}j^0 = \log K - \Delta G^0/(2.3RT) \quad (1)$$

where ΔG^0 is the reaction activation free energy, R is the gas constant, T is the temperature, and K is a factor depending on the concentration.

A lower ΔG^0 corresponds to a higher activity. The values for ΔG^0 can be extracted from the corresponding slopes for $\log j^0$ vs $1/T$ in Fig. 7(b). The ΔG^0 values obtained for the methanol oxidation are −13.55 and −13.18 kJ/mol for the Pt/CNTs-2 and Pt/CNTs-HF catalysts, respectively. This reflects an improved rate for methanol oxidation on the Pt/CNTs-2. Table 1 summarizes the exchange current densities for the methanol oxidation on both Pt/CNTs-2 and Pt/CNTs-HF.

Table 1 Comparison of the exchange current densities for methanol oxidation on Pt/CNTs-2 and Pt/CNTs-HF electrodes at different temperatures.

Temperature	Tafel slope (mV/dec)		j^o/(mA/cm^2)	
(K)	Pt/CNTs-2	Pt/CNTs-HF	Pt/CNTs-2	Pt/CNTs-HF
298	49.22	47.42	7.28×10^{-8}	6.62×10^{-9}
308	58.58	54.05	8.14×10^{-7}	4.75×10^{-8}
318	69.72	61.41	5.26×10^{-6}	3.45×10^{-6}
328	96.11	79.83	1.71×10^{-3}	7.21×10^{-6}
338	114.25	94.25	8.91×10^{-3}	7.78×10^{-4}

For the methanol oxidation, resistance to CO poisoning is also very important, since the CO-like by-products generated during the oxidation can occupy the Pt active sites and consequently decrease their activity towards the desired oxidation [23]. Linear current sweeping measurements were employed to investigate the CO poisoning-resistance for all the prepared catalysts and the corresponding results are summarized in Fig. 8. Potential oscillation is a typical phenomenon for Pt, because of poisoning by the CO-like

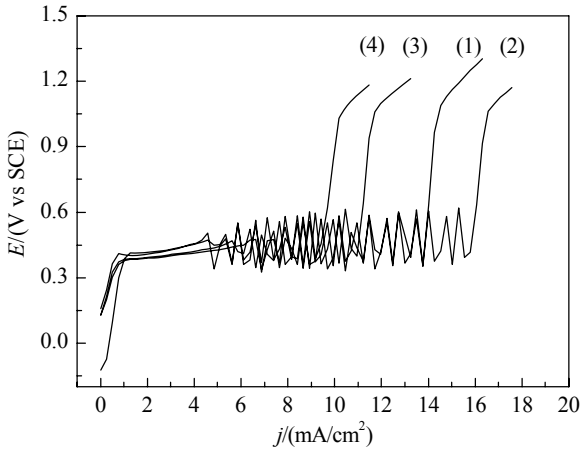

Fig. 8. The current sweep curves for the methanol oxidation on Pt/CNTs-1 (1), Pt/CNTs-2 (2), Pt/CNTs-3 (3), and Pt/CNTs-HF (4) in 0.5 mol/L aqueous H_2SO_4 + 1.0 mol/L CH_3OH at a scan rate of 50 μA/s.

by-products generated throughout the dehydrogenation of methanol. The highest potential oscillation was observed for Pt/CNTs-2, and the order for all the investigated catalysts follows the sequence of Pt/CNTs-2>Pt/CNTs-1> Pt/CNTs-3 > Pt/CNTs-HF. We believe that this high stability predominantly originates from the improved graphitization and functionalization of the CNTs. These enhance the interaction between the Pt particles and the CNTs.

To further investigate the stabilities of the catalysts, chronoamperometry measurements were used by holding the potential at 0.35 and 0.60 V for 3600 s. The changes in the oxidation current with time were recorded. As shown in Fig. 9, the oxidation currents decreased continuously for all the catalysts, presumably due to catalyst poisoning via the by-products formed throughout the oxidation of methanol. Any adsorbed SO_4^{2-} anions on the surface of the Pt could also inhibit the methanol oxidation reaction [24]. At 0.35 V, in the region of activation polarization, the Pt/CNTs-2 possess the highest current density. All the prepared catalysts follow the order of Pt/CNTs-2 > Pt/CNTs-1 > Pt/CNTs-3 > Pt/CNTs-HF. Similarly, at 0.60 V, which is approaching the region of peak potential, the Pt/CNTs-2 is also able to maintain the highest current density of all the catalysts. This further supports its superior catalytic performance. This may be attributed to the stronger metal-support interactions between the Pt particles and the CNTs.

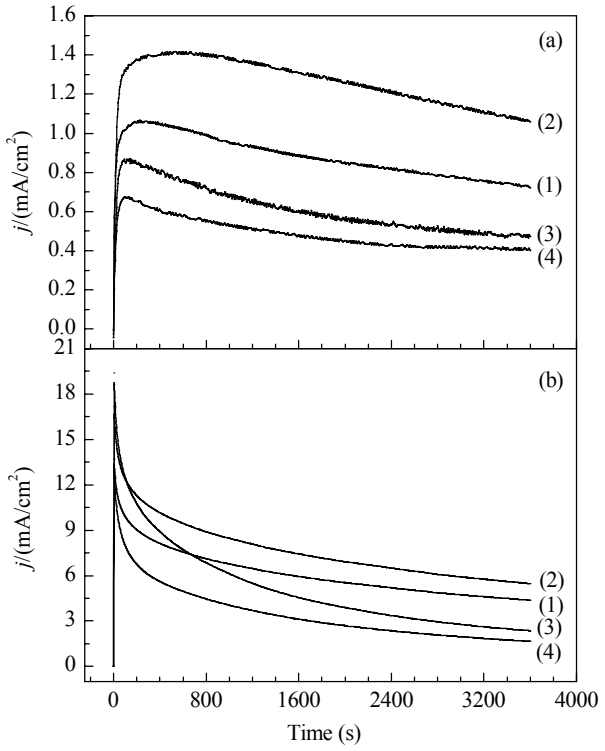

Fig. 9. Chronoamperometry curves for Pt/CNTs-1 (1), Pt/CNTs-2 (2), Pt/CNTs-3 (3), and Pt/CNTs-HF (4) in 0.5 mol/L aqueous H_2SO_4 + 1.0 mol/L CH_3OH, with the potential held at 0.35 V (a) and 0.60 V (b) at 25 ºC.

3 Conclusions

A method to efficiently functionalize CNTs as Pt catalyst supports via a combined HF corrosion and intermittent microwave heating strategy, using H_2O_2 solution, has been developed and demonstrated. The sample prepared using a 10s-on/20s-off pulsing protocol over five cycles has been employed as catalyst supports and exhibits the best activity towards methanol oxidation among those in this study. It also shows a significantly improved stability towards the methanol oxidation conditions upon comparison to the other CNTs. We believe that this high stability originates from the improved CNT modifications, which enhance the interactions between the Pt particles and the CNTs. The results represent a novel approach for the simple and economical functionalization of CNTs. The methodology could also be potentially applied in the mass production of nanosized materials due to its convenient scalability.

References

1 李莉香, 刘永长, 耿新, 安百刚. 物理化学学报(Li L X, Liu Y Ch, Geng X, An B G. *Acta Phys-Chim Sin*), 2011, **27**: 443
2 Zhang W M, Sherrell P, Minett A I, Razal J M, Chen J. *Energy Environ Sci*, 2010, **3**: 1286
3 唐水花, 孙公权, 齐静, 孙世国, 郭军松, 辛勤, Geir Martin Haarberg. 催化学报(Tang Sh H, Sun G Q, Qi J, Sun Sh G, Guo J S, Xin Q, Haarberg G M. *Chin J Catal*), 2010, **31**: 12
4 He D P, Mu S C, Pan M. *Carbon*, 2011, **49**: 82
5 He D P, Zeng C, Xu C, Cheng N C, Li H G, Mu S C, Pan M. *Langmuir*, 2011, **27**: 5582
6 Yin Sh B, Luo L, Xu C, Zhao Y L, Qiang Y H, Mu S C. *J Power Sources*, 2012, **198**: 1
7 He C X, Song S Q, Liu J C, Maragou V, Tsiakaras P. *J Power Sources*, 2010, **195**: 7409
8 Zhang J, Zou H, Qing Q, Yang Y, Li Q, Liu Z, Guo X, Du Z. *J Phys Chem B*, 2003, **107**: 3712
9 Feng L Y, Yan Y Y, Chen Y G, Wang L J. *Energy Environ Sci*, 2011, **4**: 1892
10 Jiang K Y, Eitan A, Schadler L S, Ajayan P M, Siegel R W, Grobert N, Mayne M, Reyes-Reyes M, Terrones H, Terrones M. *Nano Lett*, 2003, **3**: 275
11 Liu Z L, Lin X H, Lee J Y, Zhang W D, Han M, Gan L M. *Langmuir*, 2002, **18**: 4054
12 Liu J, Rinzler A G, Dai H, Hafner H J, Bradley R K, Boul P J, Lu A, Iverson T, Shelimov K, Huffman C B, Rodriguez-Macias F, Shon Y S, Lee T R, Colbert D T, Smalley R E. *Science*, 1998, **280**: 1253
13 Hu F P, Shen P K, Li Y L, Liang J Y, Wu J, Bao Q L, Li C M, Wei Z D. *Fuel Cells*, 2008, **8**: 429
14 Li Y L, Hu F P, Wang X, Shen P K. *Electrochem Commun*,

2008, **10**: 1101
15 Shen P K, Yin Sh B, Li Z H, Chen C. *Electrochim Acta*, 2010, **55**: 7969
16 Yin Sh B, Cai M, Wang C X, Shen P K. *Energy Environ Sci*, 2011, **4**: 558
17 Yin Sh B, Shen P K, Song S Q, Jiang S P. *Electrochim Acta*, 2009, **54**: 6954
18 Song S Q, Wang Y, Shen P K. *J Power Sources*, 2007, **170**: 46
19 Patterson A L. *Phys Rev*, 1939, **56**: 978
20 Xing Y C, Li L, Chusuei C C, Hull R V. *Langmuir*, 2005, **21**: 4185
21 Wu J, Hu F P, Shen P K, Li C M, Wei Z D. *Fuel Cells*, 2010, **10**: 106
22 Wu J, Hu F P, Hu X D, Wei Z D, Shen P K. *Electrochim Acta*, 2008, **53**: 8341
23 Zhao Z Z, Fang X, Li Y L, Wang Y, Shen P K, Xie F Y, Zhang X. *Electrochem Commun*, 2009, **11**: 290
24 Xu W L, Shen H, Kim Y J, Zhou X C, Liu G K, Park J, Chen P. *Nano Lett*, 2009, **9**: 3968